Synchronization transition of a coupled system composed of neurons with coexisting behaviors near a Hopf bifurcation*

Jia Bing(贾 冰)†

Center for Computational System Biology, School of Mathematical Science, Fudan University, Shanghai 200433, *China*

(Received 6 September 2013; revised manuscript received 29 October 2013; published online 25 March 2014)

The coexistence of a resting condition and period-1 firing near a subcritical Hopf bifurcation point, lying between the monostable resting condition and period-1 firing, is often observed in neurons of the central nervous systems. Near such a bifurcation point in the Morris–Lecar (ML) model, the attraction domain of the resting condition decreases while that of the coexisting period-1 firing increases as the bifurcation parameter value increases. With the increase of the coupling strength, and parameter and initial value dependent synchronization transition processes from non-synchronization to compete synchronization are simulated in two coupled ML neurons with coexisting behaviors: one neuron chosen as the resting condition and the other the coexisting period-1 firing. The complete synchronization is either a resting condition or period-1 firing dependent on the initial values of period-1 firing when the bifurcation parameter value is small or middle and is period-1 firing when the parameter value is large. As the bifurcation parameter value increases, the probability of the initial values of a period-1 firing neuron that lead to complete synchronization of period-1 firing increases, while that leading to complete synchronization of the resting condition decreases. It shows that the attraction domain of a coexisting behavior is larger, the probability of initial values leading to complete synchronization of this behavior is higher. The bifurcations of the coupled system are investigated and discussed. The results reveal the complex dynamics of synchronization behaviors of the coupled system composed of neurons with the coexisting resting condition and period-1 firing, and are helpful to further identify the dynamics of the spatiotemporal behaviors of the central nervous system.

Keywords: synchronization, neuronal network, Hopf bifurcation, coexistence

PACS: 05.45.Xt, 87.18.Tt, 87.18.Hf **DOI:** 10.1088/1674-1056/23/5/050510

1. Introduction

Spatio-temporal behavior is ubiquitous in nature and spreads all over fields such as biology, ecology, physics, sociology, and so on.[1–12] Synchronization in nervous systems such as the mammalian visual cortex, the human thalamocortical area and the stomatogastric ganglion of the spiny lobster,[13–15] which is the collective behavior of interacting neurons or functional units, has been paid much attention. Synchronization behaviors play important roles in information processing and motion coordination, such as the visual sense and learning, cognition, perception and movement control.[13–19] Moreover, the transition between different synchronization patterns induced by the difficulty degree of oddball tasks in visual sensing[20] and auditory sensing[17] were observed. Identification of the dynamics of synchronization and synchronization transition in coupled systems is very important for neuroscience.

In recent years, the investigation of synchronization has been extended from monostable dynamical systems to multistable dynamical systems.[21–23] As is well known, a single neuron can exhibit the resting condition or firings that can be roughly classified into spiking and bursting patterns.[24] Recently, coexisting behaviors, as a representative nonlinear phenomenon, have been widely studied in real nervous systems and theoretical models, which is due to the potential functions as mechanisms for memory storage or information processing.[24–36] The coexistence of the resting condition and period-1 firing, of the bursting and spiking, and of the period-1 bursting and period-2 bursting was simulated in many models with sub-critical Andronov–Hopf,[24,27] in a cortical neuron model and a leech neuron model,[28–30] and in the Chay model,[31,32] respectively, and experimentally demonstrated in an axon,[35] in neuron R15 of aplysia[36] and in an experimental neural pacemaker,[31,32] respectively. Theoretically, the coexistence of the resting condition and period-1 firing appears near a sub-critical Hopf bifurcation point, which has been related to the type II excitability in the nervous system.[24,27] Type II excitability or Hopf bifurcation has been simulated in several theoretical models and observed in real nervous systems, especially in the central nervous systems,[33,37,38] for example, neurons in layers of 2/3 of slices of somatosensory cortex and CA1 hippocampal pyramidal neurons of a rat. Other than type II excitability, type I excitability and saddle-node bifurcation is another popular phenomenon near a threshold observed in nervous systems.[34] In this paper, we focus on a subcritical Hopf bifurcation point.

The synchronization behaviors of a coupled system with coexisting behaviors are as follows. Different synchronization states, such as the intermittent, phase, and anticipated synchro-

*Project supported by the National Natural Science Foundation of China (Grant No. 11072135).

†Corresponding author. E-mail: jiabing427@163.com; jiabing427@gmail.com

© 2014 Chinese Physical Society and IOP Publishing Ltd

nization, were observed in two undirectionally coupled identical systems with coexisting chaotic attractors.[39] Synchronization of unidirectionally coupled optical bistable systems with coexisting attractors (fixed point and chaos, fixed point and one periodic orbit, and two periodic orbits with different periods) was reported.[39] Recently, synchronization transition has been simulated in two coupled leech neurons with coexisting spiking and bursting.[28,40] The two coupled neurons manifest different synchronization transition process with the increase of the coupling strength when the two neurons were chosen as different combinations of bursting or spiking patterns. When one neuron was spiking and the other coexisting was bursting, complete synchronization of spiking was simulated when the coupling strength was strong.[28] In a recent study, the complete synchronization corresponding to strong coupling strength was further identified to be either spiking or bursting, which is dependent on the bifurcation parameter that controls the coexisting behaviors.[40] These investigations provided a primary evaluation of two coupled neurons with coexisting spiking and bursting.

In the present study, we employ the Morris–Lecar neuron model with coexistence of the resting condition and period-1 firing near a sub-critical Hopf bifurcation point,[27] and pay attention to the parameter-dependent synchronization transition processes with respect to the coupling strength and initial value-dependent complete synchronization of the two coupled ML neurons. As the first step, the coupled system with only two neurons is investigated. The results indicate that the two coupled neurons with coexisting behaviors can exhibit different synchronization transition processes dependent on the bifurcation parameter values and initial value-dependent complete synchronization corresponding to strong coupling strength. The present paper provides a particular study of synchronization behaviors of the two coupled neurons with coexisting behaviors of the resting condition and period-1 firing.

2. Morris–Lecar (ML) model and the coexisting behaviors

2.1. ML model

The ML model, a well-known conductance-based neuron model, has been frequently employed in the studies of Hopf bifurcation and saddle-node bifurcation, and of neuronal networks.[7–12] The ML model is as follows:[27]

$$\frac{\mathrm{d}V}{\mathrm{d}t} = \frac{1}{C}[-g_{\mathrm{l}}(V-v_{\mathrm{l}}) - g_{\mathrm{Ca}}m_{\infty}(V)(V-v_{\mathrm{Ca}}) - g_{\mathrm{k}}\omega(V-v_{\mathrm{k}}) + I], \tag{1a}$$

$$\frac{\mathrm{d}\omega}{\mathrm{d}t} = \phi\frac{\omega_{\infty}(V)-\omega}{\tau_{\omega}(V)}. \tag{1b}$$

Here, t is time; V is the membrane potential; ω represents the recovery variable; C is the membrane capacitance; I is the background current; g_{Ca}, g_{k}, and g_{l} are maximal conductance for corresponding ionic currents and leakage current, respectively; v_{Ca}, v_{k}, and v_{l} are the corresponding reversal potential, respectively; m_{∞}, ω_{∞}, and τ_{ω} are the steady-state calcium, potassium activation, and the rate constant of potassium ionic channel open probability, respectively. They are functions of V defined as: $m_{\infty}(V) = 0.5\{1+\tanh[(V-v_1)/v_2]\}$, $\omega_{\infty}(V) = 0.5\{1+\tanh[(V-v_3)/v_4]\}$, $\tau_{\omega}(V) = 1/\{\cosh[(V-v_3)/2v_4]\}$, respectively. The units of time, voltage and current are ms, mV, and μA, respectively. The ML model is solved by the 4-th Runge–Kutta integration method with time step of 0.1 ms.

In the present paper, the parameter values are as follows: $C = 20$ μF/cm^2, $g_{\mathrm{Ca}} = 4.4$ mS/cm^2, $g_{\mathrm{k}} = 8.0$ mS/cm^2, $g_{\mathrm{l}} = 2.0$ mS/cm^2, $v_{\mathrm{Ca}} = 120$ mV, $v_{\mathrm{k}} = -84$ mV, $v_{\mathrm{l}} = -60$ mV, $v_1 = -1.2$ mV, $v_2 = 18$ mV, $v_3 = 2$ mV, $v_4 = 30$ mV, and $\phi = 0.04$.

2.2. Bifurcations and coexisting behaviors of the ML model

As pointed out in a previous study,[27] the ML model with parameter values used in this paper manifests a unique equilibrium whose values are dependent on I. Firstly, we calculate equilibrium denoted by $E_0(V_0, \omega_0)$ satisfying

$$\frac{1}{C}[-g_{\mathrm{l}}(V_0-v_{\mathrm{l}}) - g_{\mathrm{Ca}}m_{\infty}(V_0)(V_0-v_{\mathrm{Ca}}) - g_{\mathrm{k}}\omega_0(V_0-v_{\mathrm{k}}) + I] = 0, \tag{2a}$$

$$\phi\frac{\omega_{\infty}(V_0)-\omega_0}{\tau_{\omega}(V_0)} = 0. \tag{2b}$$

Equations (2a) and (2b) can be simplified into equations as follows:

$$-g_{\mathrm{l}}(V_0-v_{\mathrm{l}}) - g_{\mathrm{Ca}}m_{\infty}(V_0)(V_0-v_{\mathrm{Ca}}) - g_{\mathrm{k}}\omega_0(V_0-v_{\mathrm{k}}) + I = 0, \tag{3a}$$

$$\omega_0 = \omega_{\infty}(V_0). \tag{3b}$$

Substituting Eq. (3a) into Eq. (3b), we can acquire a nonlinear equation

$$-g_{\mathrm{l}}(V_0-v_{\mathrm{l}}) - g_{\mathrm{Ca}}m_{\infty}(V_0)(V_0-v_{\mathrm{Ca}}) - g_{\mathrm{k}}\omega_{\infty}(V_0)(V_0-v_{\mathrm{k}}) + I = 0. \tag{4}$$

We introduce a function

$$f(V) = -g_{\mathrm{l}}(V-v_{\mathrm{l}}) - g_{\mathrm{Ca}}m_{\infty}(V)(V-v_{\mathrm{Ca}}) - g_{\mathrm{k}}\omega_{\infty}(V)(V-v_{\mathrm{k}}) + I. \tag{5}$$

The value of $\mathrm{d}f(V)/\mathrm{d}V$, i.e., the derivative of function $f(V)$, is negative when V is between -200 mV and 200 mV, as shown in Fig. 1(a) ($I = 89.5$) , showing that $f(V)$ monotonically decreases with respect to the increase of V, as shown in Fig. 1(b) ($I = 89.5$). Because I is a constant, the value of $f(V)$ is dependent on I while the monotonically decreasing characteristic of $f(V)$ is independent of I.

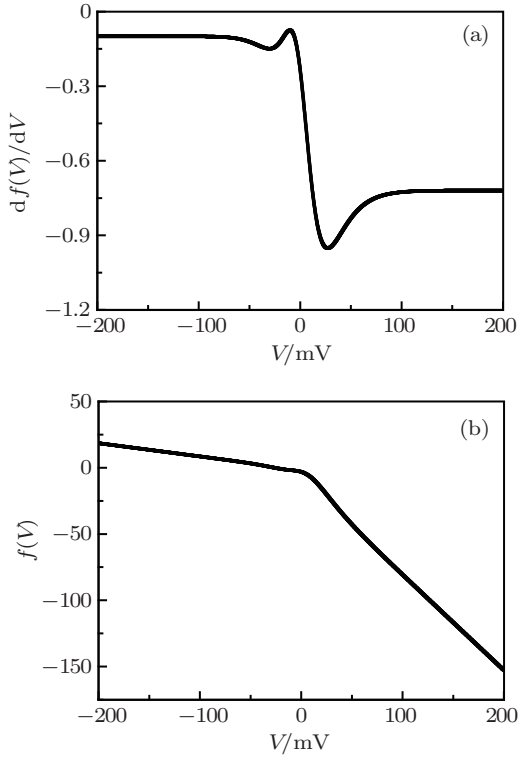


Fig. 1. (a) Changes of derivative of function $f(V)$ with respect to V when $I = 89.5$; (b) changes of $f(V)$ with respect to V when $I = 89.5$.

For a given value of I, V_0 is the root of $f(V) = 0$, and $\omega_0 = \omega_\infty(V_0)$. For example, when $I = 88.4$, $V_0 = -27.14102$, $\omega_0 = 0.12535$; when $I = 89.5$, $V_0 = -26.76724$, $\omega_0 = 0.12811$; when $I = 93$, $V_0 = -25.56721$, $\omega_0 = 0.13731$. The change of V_0 with respect to I is shown by the thin solid and thin dotted line in Fig. 2.

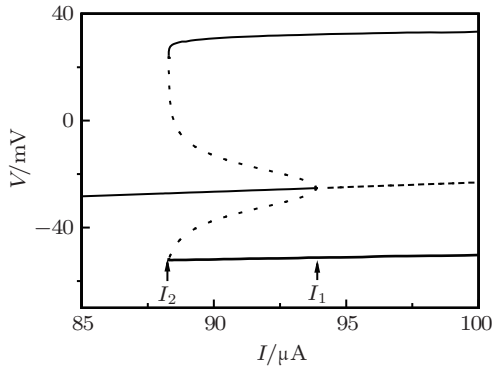


Fig. 2. The bifurcation structure of the ML model with respect to I near a sub-critical Hopf bifurcation point.

Secondly, we calculate the stability of the equilibrium E_0. We linearize the ML model near E_0 with a fixed I value and the corresponding Jacobian matrix $\boldsymbol{B}$ is written as

$$\begin{aligned}\boldsymbol{B} = \begin{pmatrix} a_{11} & a_{12} \\ a_{21} & a_{22} \end{pmatrix} &= \begin{pmatrix} \frac{1}{C}\left[-g_{\rm l} - g_{\rm Ca} m_\infty(V) - g_{\rm Ca}(V - v_{\rm Ca})\frac{\partial m_\infty(V)}{\partial V} - g_{\rm k}\omega\right] & \frac{1}{C}[-g_{\rm k}(V - v_{\rm k})] \\ -\frac{\phi(-\omega + \omega_\infty(V))}{\tau_\omega(V)^2}\frac{\partial \tau_\omega(V)}{\partial V} + \frac{\phi}{\tau_\omega(V)}\frac{\partial \omega_\infty(V)}{\partial V} & -\frac{\phi}{\tau_\omega} \end{pmatrix} \Bigg| E_0 \\ &= \begin{pmatrix} \frac{1}{C}\left[-g_{\rm l} - g_{\rm Ca} m_\infty(V_0) - g_{\rm Ca}(V_0 - v_{\rm Ca})\frac{\partial m_\infty(V_0)}{\partial V} - g_{\rm k}\omega_0\right] & \frac{1}{C}[-g_{\rm k}(V_0 - v_{\rm k})] \\ -\frac{\phi(-\omega_0 + \omega_\infty(V_0))}{\tau_\omega^2(V_0)}\frac{\partial \tau_\omega(V_0)}{\partial V} + \frac{\phi}{\tau_\omega(V_0)}\frac{\partial \omega_\infty(V_0)}{\partial V} & -\frac{\phi}{\tau_\omega(V_0)} \end{pmatrix} \\ &= \begin{pmatrix} \frac{1}{C}\left[-g_{\rm l} - g_{\rm Ca} m_\infty(V_0) - g_{\rm Ca}(V_0 - v_{\rm Ca})\frac{\partial m_\infty(V_0)}{\partial V} - g_{\rm k}\omega_0\right] & \frac{1}{C}[-g_{\rm k}(V_0 - v_{\rm k})] \\ \frac{\phi}{\tau_\omega(V_0)}\frac{\partial \omega_\infty(V_0)}{\partial V} & -\frac{\phi}{\tau_\omega(V_0)} \end{pmatrix}.\end{aligned}$$

The characteristic polynomial of matrix $\boldsymbol{B}$ is given by

$$\begin{aligned} f_{\boldsymbol{B}}(\lambda) &= |\lambda \boldsymbol{I} - \boldsymbol{B}| = \begin{vmatrix} \lambda - a_{11} & -a_{12} \\ -a_{21} & \lambda - a_{22} \end{vmatrix} \\ &= \lambda^2 + (-a_{11} - a_{22})\lambda + (a_{11}a_{22} - a_{12}a_{21}). \quad (6) \end{aligned}$$

If roots of $f_{\boldsymbol{B}}(\lambda) = 0$, labeled as λ_1 and λ_2, are negative real numbers or complex numbers with negative real parts, correspondingly, the equilibrium E_0 is a stable node or a stable focus. For example, when $I = 88.4$,

$$\begin{pmatrix} a_{11} & a_{12} \\ a_{21} & a_{22} \end{pmatrix} = \begin{pmatrix} 0.0188279 & -22.7436 \\ 0.000327527 & -0.0448112 \end{pmatrix},$$

$\lambda_{1,2} = -0.0130 \pm 0.0802\mathrm{i}$; when $I = 89.5$,

$$\begin{pmatrix} a_{11} & a_{12} \\ a_{21} & a_{22} \end{pmatrix} = \begin{pmatrix} 0.0235971 & -22.8931 \\ 0.000332747 & -0.0446863 \end{pmatrix},$$

$\lambda_{1,2} = -0.0105 \pm 0.0803\mathrm{i}$; when $I = 93$,

$$\begin{pmatrix} a_{11} & a_{12} \\ a_{21} & a_{22} \end{pmatrix} = \begin{pmatrix} 0.0399195 & -23.3731 \\ 0.000349814 & -0.0442967 \end{pmatrix},$$

$\lambda_{1,2} = -0.0022 \pm 0.0800\mathrm{i}$. The equilibria corresponding to $I = 88.4$, 89.5, and 93 are all stable focuses.

An alternative method to analyze the stability of equilibrium E_0 is to calculate the trace $(a_{11} + a_{22})$ and determinant $(a_{11}a_{22} - a_{12}a_{21})$ of the matrix $\boldsymbol{B}$. The necessary and sufficient condition that E_0 is stable is $a_{11} + a_{22} < 0$

and $a_{11}a_{22} - a_{12}a_{21} > 0$. The matrices $\boldsymbol{B}$ corresponding to $I = 88.4$, 89.5, and 93 satisfy this condition.

Through calculation of the eigenvalues of Jacobian matrix $\boldsymbol{B}$ with respect to I, a sub-critical Hopf bifurcation point of E_0 happens near $I = I_1 \approx 93.86$. When $I < I_1$, E_0 is a stable focus, as shown by the thin solid line in Fig. 2. When $I > I_1$, E_0 is an unstable focus, as shown by the thin dotted line in Fig. 2. An unstable periodic orbit appears at $I = I_1$, as illustrated by the dashed lines in Fig. 2. The upper (lower) dashed line represents the maximum (minimal) value of the unstable limit cycle. With decreasing I, the amplitude of the unstable limit cycle increases. When $I = I_2 \approx 88.29$, a fold bifurcation of the limit cycle appears. The unstable limit cycle and a stable limit cycle merges and disappears. When $I > I_2$, the stable limit cycle appears as a period-1 firing, as shown by the bold solid lines in Fig. 2. The upper (lower) bold solid line represents the maximum (minimal) value of the stable limit cycle.

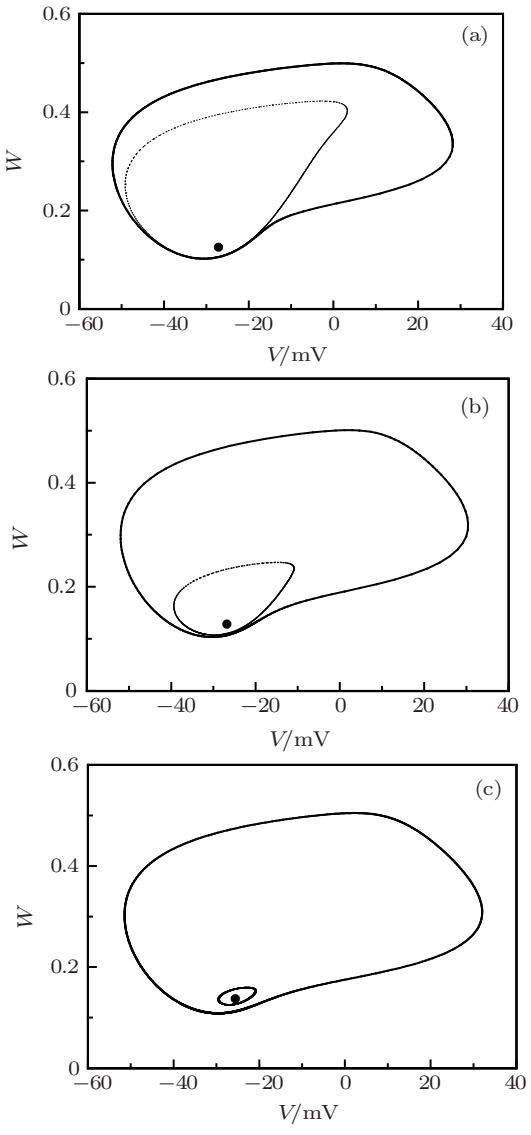


Fig. 3. The trajectory of the stable limit cycle (solid line), the unstable limit cycle (dotted line), and the stable focus (circle point) at different I values: (a) $I = 88.4$; (b) $I = 89.5$; (c) $I = 93$.

When $I_2 < I < I_1$, a stable focus, an unstable limit cycle, and a stable limit cycle coexist. The stable focus corresponds to the resting condition and the stable limit cycle corresponds to the period-1 firing. The bifurcation structure is shown in Fig. 2. The unstable limit cycle is the border separating the attraction basins of the stable focus and the stable limit cycle. The coexistence structures in the (V, ω) plane corresponding to $I = 88.4$, 89.5, and 93 are shown in Figs. 3(a)–3(c). If the initial values of V and ω are chosen to be located outside the unstable limit cycle, the system will evolve to and stay along the stable limit cycle. If the initial values of V and ω are inside the unstable limit cycle, the system will evolve to the stable focus. With I increasing, the attraction domain of the stable focus (resting condition) decreases while that of the stable limit cycle (period-1 firing) increases. In the present study, the synchronization behaviors of the two coupled neurons corresponding to $I = 88.4$, 89.5, and 93 are investigated in the following sections.

3. Model of the two coupled neurons

3.1. Model

The model composed of two coupled ML neurons is as follows:

$$\frac{dV_1}{dt} = \frac{1}{C}[-g_l(V_1 - v_l) - g_{Ca}m_\infty(V_1)(V_1 - v_{Ca}) - g_k\omega_1(V_1 - v_k) + I] + g_c(V_2 - V_1), \tag{7a}$$

$$\frac{d\omega_1}{dt} = \phi\frac{\omega_\infty(V_1) - \omega_1}{\tau_\omega(V_1)}, \tag{7b}$$

$$\frac{dV_2}{dt} = \frac{1}{C}[-g_l(V_2 - v_l) - g_{Ca}m_\infty(V_2)(V_2 - v_{Ca}) - g_k\omega_2(V_2 - v_k) + I] + g_c(V_1 - V_2), \tag{7c}$$

$$\frac{d\omega_2}{dt} = \phi\frac{\omega_\infty(V_2) - \omega_2}{\tau_\omega(V_2)}. \tag{7d}$$

Here, the subscripts 1 and 2 are respectively used to indicate the neuron with resting condition (labeled as neuron 1) and with period-1 firing (neuron 2), g_c is the coupling strength between neurons 1 and 2. In this paper, $g_c \geq 0$.

3.2. Bifurcations of equilibrium of the coupled system with respect to g_c

3.2.1. Bifurcations of equilibrium related to E_0

When $E_0(V_0, \omega_0)$ is an equilibrium of a single neuron model, we can easily identify that $(V_0, \omega_0, V_0, \omega_0)$ is an equilibrium of the coupled system described by Eqs. 7(a)–7(c). The equilibrium $(V_0, \omega_0, V_0, \omega_0)$ is labeled as E_{00}, related to the E_0 of the single neuron model.

To determine the stability of equilibrium E_{00}, we linearize the coupled system near E_{00}, and the corresponding Jacobian

matrix $\boldsymbol{A}$ can be written as

$$\boldsymbol{A}=\begin{pmatrix} a_{11}-g_{\rm c} & a_{12} & g_{\rm c} & 0 \\ a_{21} & a_{22} & 0 & 0 \\ g_{\rm c} & 0 & a_{11}-g_{\rm c} & a_{12} \\ 0 & 0 & a_{21} & a_{22} \end{pmatrix}.$$

The characteristic polynomial is given by

$$\begin{aligned} f_{\boldsymbol{A}}(\lambda) &= |\lambda \boldsymbol{I}-\boldsymbol{A}| \\ &= \begin{vmatrix} \lambda-(a_{11}-g_{\rm c}) & -a_{12} & -g_{\rm c} & 0 \\ -a_{21} & \lambda-a_{22} & 0 & 0 \\ -g_{\rm c} & 0 & \lambda-(a_{11}-g_{\rm c}) & -a_{12} \\ 0 & 0 & -a_{21} & \lambda-a_{22} \end{vmatrix} \\ &\triangleq \begin{vmatrix} \boldsymbol{C} & -g_{\rm c}\boldsymbol{\Gamma} \\ -g_{\rm c}\boldsymbol{\Gamma} & \boldsymbol{C} \end{vmatrix}, \end{aligned}$$

where

$$\boldsymbol{C}=\begin{pmatrix} \lambda-(a_{11}-g_{\rm c}) & -a_{12} \\ -a_{21} & \lambda-a_{22} \end{pmatrix}, \quad \boldsymbol{\Gamma}=\begin{pmatrix} 1 & 0 \\ 0 & 0 \end{pmatrix}.$$

According to the theory of blocked determination, we obtain

$$\begin{aligned} f_{\boldsymbol{A}}(\lambda) &= |\boldsymbol{C}^2-g_{\rm c}^2\boldsymbol{\Gamma}| = |\boldsymbol{C}-g_{\rm c}\boldsymbol{\Gamma}|\cdot|\boldsymbol{C}+g_{\rm c}\boldsymbol{\Gamma}| \\ &\triangleq \Delta_1(\lambda)\Delta_2(\lambda), \end{aligned}$$

where

$$\begin{aligned} \Delta_1(\lambda) &= |\boldsymbol{C}-g_{\rm c}\boldsymbol{\Gamma}| = \begin{vmatrix} \lambda-a_{11} & -a_{12} \\ -a_{21} & \lambda-a_{22} \end{vmatrix} \\ &= \lambda^2+(-a_{11}-a_{22})\lambda+a_{11}a_{22}-a_{12}a_{21}, \\ \Delta_2(\lambda) &= |\boldsymbol{C}+g_{\rm c}\boldsymbol{\Gamma}| = \begin{vmatrix} \lambda-a_{11}+2g_{\rm c} & -a_{12} \\ -a_{21} & \lambda-a_{22} \end{vmatrix} \\ &= \lambda^2+(-a_{11}-a_{22}+2g_{\rm c})\lambda \\ &\quad +a_{11}a_{22}-a_{12}a_{21}-2a_{22}g_{\rm c}. \end{aligned}$$

Theorem 1 If E_0 of the single neuron model is stable and $g_{\rm c}\geq 0$, then E_{00} of the coupled system is stable. It is equivalent to that if $a_{11}+a_{22}<0$ and $a_{11}a_{22}-a_{12}a_{21}>0$, then $a_{11}+a_{22}-2g_{\rm c}<0$ and $a_{11}a_{22}-a_{12}a_{21}-2a_{22}g_{\rm c}>0$.

Proof Firstly, it is noticed that $\Delta_1(\lambda)=f_{\boldsymbol{B}}(\lambda)$ and $\Delta_1(\lambda)$ is independent of $g_{\rm c}$. Therefore, $\Delta_1(\lambda)$ and $f_{\boldsymbol{B}}(\lambda)=0$ of matrix $\boldsymbol{B}$ have identical eigenvalues λ_1 and λ_2. If E_0 is stable, λ_1 and λ_2 of $\Delta_1(\lambda)=0$ are also negative real numbers or complex numbers with negative real parts.

Secondly, the roots of $\Delta_2(\lambda)=0$ can be identified as negative real numbers or complex numbers with negative real parts, $\Delta_2(\lambda)$ is the characteristic polynomial of a matrix labeled as

$$\boldsymbol{D}=\begin{pmatrix} a_{11}-2g_{\rm c} & a_{12} \\ a_{21} & a_{22} \end{pmatrix},$$

where $a_{22}=-\phi/\tau_\omega(V)<0$, because $\phi=0.04>0$ and $\tau_\omega(V)=1/\{\cosh[(V-v_3)/2v_4]\}^{-1}>0$. In the present study, $g_{\rm c}\geq 0$, therefore, the trace and determinant of matrix D are as follows:

$$a_{11}+a_{22}-2g_{\rm c}\leq a_{11}+a_{22}<0, \tag{8a}$$

$$a_{11}a_{22}-a_{12}a_{21}-2a_{22}g_{\rm c}>a_{11}a_{22}-a_{12}a_{21}>0. \tag{8b}$$

Therefore, λ_1 and λ_2 of $\Delta_2(\lambda)$ are also negative real numbers or complex numbers with negative real parts.

Combined λ_1 and λ_2 of $\Delta_1(\lambda)$ and $\Delta_2(\lambda)$, the equilibrium E_{00} of the coupled system is stable when the corresponding equilibrium E_0 of the single neuron model is stable and $g_{\rm c}>0$. The result shows that no bifurcation happens in E_{00} when $I=88.4$, 89.5, and 93 with respect to $g_{\rm c}$ when $g_{\rm c}>0$.

3.2.2. No other equilibrium different from E_{00}

It is an important characteristic that the coupled system is invariant if indices 1 and 2 are interchanged. Therefore, if (V_{10}, ω_{10}, V_{20}, ω_{20}) is a root of the coupled system, then (V_{20}, ω_{20}, V_{10}, ω_{10}) will be a root of the coupled system. We consider the existence of (V_{10}, ω_{10}, V_{20}, ω_{20}) satisfying:

$$\begin{aligned} &\frac{1}{C}[-g_{\rm l}(V_{10}-v_{\rm l})-g_{\rm Ca}m_\infty(V_{10})(V_{10}-v_{\rm Ca}) \\ &-g_{\rm k}\omega_{10}(V_{10}-v_{\rm k})+I]+g_{\rm c}(V_{20}-V_{10})=0, \end{aligned} \tag{9a}$$

$$\phi\frac{\omega_\infty(V_{10})-\omega_{10}}{\tau_\omega(V_{10})}=0, \tag{9b}$$

$$\begin{aligned} &\frac{1}{C}[-g_{\rm l}(V_{20}-v_{\rm l})-g_{\rm Ca}m_\infty(V_{20})(V_{20}-v_{\rm Ca}) \\ &-g_{\rm k}\omega_{20}(V_{20}-v_{\rm k})+I]+g_{\rm c}(V_{10}-V_{20})=0, \end{aligned} \tag{9c}$$

$$\phi\frac{\omega_\infty(V_{20})-\omega_{20}}{\tau_\omega(V_{20})}=0. \tag{9d}$$

Substitute Eq. (9b) into Eq. (9a), and Eq. (9d) into Eq. (9c), two equations are obtained as follows:

$$\begin{aligned} &\frac{1}{C}[-g_{\rm l}(V_{10}-v_{\rm l})-g_{\rm Ca}m_\infty(V_{10})(V_{10}-v_{\rm Ca}) \\ &-g_{\rm k}\omega_\infty(V_{10})(V_{10}-v_{\rm k})+I] \\ &+g_{\rm c}(V_{20}-V_{10})=0, \end{aligned} \tag{10a}$$

$$\begin{aligned} &\frac{1}{C}[-g_{\rm l}(V_{20}-v_{\rm l})-g_{\rm Ca}m_\infty(V_{20})(V_{20}-v_{\rm Ca}) \\ &-g_{\rm k}\omega_\infty(V_{20})(V_{20}-v_{\rm k})+I] \\ &+g_{\rm c}(V_{10}-V_{20})=0. \end{aligned} \tag{10b}$$

We label $\Delta V=V_{20}-V_{10}$, considering the function $f(V)$ labeled as Eq. (5), Eqs. (10a) and (10b) can be written as

$$f(V_{10})+g_{\rm c}\Delta V=0, \tag{11a}$$

$$f(V_{20})-g_{\rm c}\Delta V=0. \tag{11b}$$

By taking the sum and difference of Eqs. 11(a) and 11(b), the equations can be obtained as follows:

$$f(V_{10})+f(V_{10}+\Delta V)=0, \tag{12a}$$

$$f(V_{10}+\Delta V)-f(V_{10})=2g_{\rm c}\Delta V. \tag{12b}$$

For a given value of ΔV, V_{10} can be acquired from the first Eq. (12a), and then the corresponding $g_{\rm c}$ can be acquired from Eq. (12b). Label $Y(\Delta V)=f(V_{10}+\Delta V)-f(V_{10})$. Based on

the fact that $f(V)$ is a monotonically decreasing function, we can acquire

$$Y(\Delta V) = f(V_{10}+\Delta V) - f(V_{10}) > 0, \quad \Delta V < 0, \quad (13a)$$

$$Y(\Delta V) = f(V_{10}+\Delta V) - f(V_{10}) < 0, \quad \Delta V > 0, \quad (13b)$$

$$Y(\Delta V) = f(V_{10}+\Delta V) - f(V_{10}) = 0, \quad \Delta V = 0. \quad (13c)$$

The curve of function $Y(\Delta V)$ in the plane $(\Delta V, Y)$ passes through the second quadrant, origin of coordinates ($\Delta V = 0$, $Y = 0$) and the fourth quadrant. The function $2g_c\Delta V$ is a linear line passing through the origin ($\Delta V = 0, Y = 0$) and with a slope being as $2g_c$. For example, the curve of function $Y(\Delta V)$ when $I = 89.5$ is shown by the bold solid curve in Fig. 4. Two lines of function $2g_c\Delta V$, one with a positive slope ($g_c = 0.05$) and the other a negative slope ($g_c = -0.07$), are shown by the thin solid lines in Fig. 4.

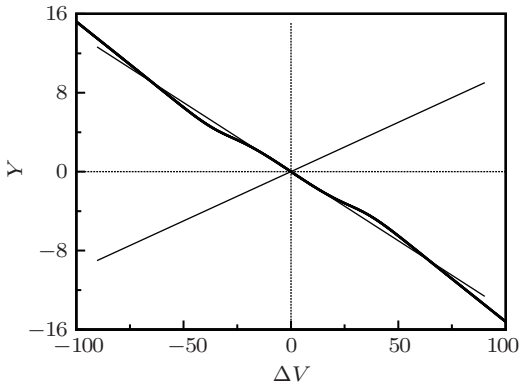


Fig. 4. Changes of function Y with respect to ΔV when $I = 93$.

The intersection points of the linear line corresponding to the function $2g_c\Delta V$ and the curve of the function $Y(\Delta V)$, i.e., the root of Eq. (12b), are related to equilibria of the coupled system. The intersection point ($\Delta V = 0$, $Y = 0$, i.e., the origin) that exists for all g_c corresponds to the equilibrium E_{00} ($\Delta V = 0, V_{10} = V_{20}$), which has been investigated particularly. With the exception of E_{00}, there exist equilibria that are different from E_{00} only when $g_c < 0$. For example, there exist four equilibria that are different from E_{00} when $g_c = -0.07$. In the present study, we do not address the equilibria and bifurcations when $g_c < 0$. When $g_c > 0$, with exception of the origin, there exist no other intersection points of the curve of the function Y and the liner line of the function $2g_c\Delta V$, showing that with the exception of E_{00}, no other equilibrium appears in the coupled system.

3.3. Criteria for synchronization degree

To characterize the synchronization degree of the two coupled neurons, a cross-correlation coefficient of the membrane potential of the two neurons (ρ) is introduced as follows:[28,40]

$$\rho = \frac{\sum_{k=1}^{N}[(V_1^k - \langle V_1^k\rangle)(V_2^k - \langle V_2^k\rangle)]}{\left[\sum_{k=1}^{N}(V_1^k - \langle V_1^k\rangle)^2 \sum_{k=1}^{N}(V_2^k - \langle V_2^k\rangle)^2\right]^{1/2}}, \quad (14)$$

where V_1^k (V_2^k) represents the samples of the membrane potential $V_1(t)$ ($V_2(t)$), $k = 1, \ldots, N$ (N represents the total number of samples), and $\langle\cdot\rangle$ denotes the average over the number of samples.

The larger the cross-correlation coefficient ρ, the higher the correlation degree between the two coupled neurons. In general, $|\rho|$ <0.8, 0.8≤ $|\rho|$ < 1, and $|\rho|$ =1 represent low, high, and complete correlations, respectively.[40] In this paper, the larger ρ, the more synchronization of the two coupled neurons. In the present study, the degrees of ρ are divided into $\rho < 0.8$, $0.8 \leq \rho < 1$, and $\rho = 1$, employed to describe different synchronization degrees, non-synchronization, nearly synchronization, and complete synchronization, respectively.

4. Synchronization states and synchronization transitions in the coupled neurons

4.1. $I = 88.4$

Synchronization behaviors of the two coupled neurons corresponding to $I = 88.4$ are investigated. The stable values of V and ω of the stable focus are -27.14102 and 0.12535, respectively.

4.1.1. Synchronization transition to complete synchronization of period-1 firing

When the initial values of the resting and period-1 firing neurons are taken as (-27.14102, 0.12535) and (1.36163, 0.21568), respectively, the two coupled neurons manifest the transition from non-synchronization (0< $g_c \leq 0.0005$), to complete synchronization of the resting condition ($0.0005 < g_c \leq 0.04$), and to complete synchronization of period-1 firing ($0.04 < g_c \leq 1$) with g_c increasing, as shown in Fig. 5.

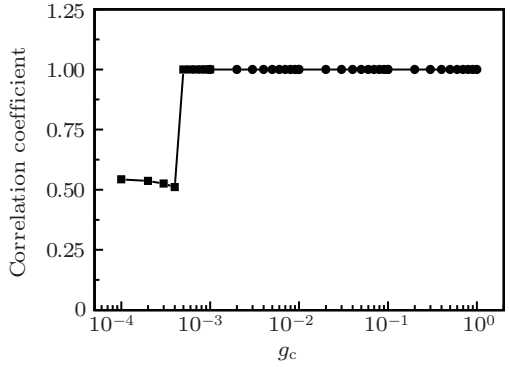


Fig. 5. Correlation coefficient between the two coupled neurons with initial values (-27.14102, 0.12535) and (1.36163, 0.21568) with g_c increasing when $I = 88.4$.

The two coupled neurons manifest non-synchronization with $\rho = 0.53$ when $g_c = 0.0003$, as shown in Fig. 6(a). Neuron 1 exhibits subthreshold oscillation and neuron 2 manifests firing. When $g_c = 0.03$, the two coupled neurons manifest complete synchronization of the resting condition, as shown in Fig. 6(b). When $g_c = 0.5$, the coupled neurons exhibit complete synchronization of period-1 firing with $\rho = 1$, as shown in Fig. 6(c).

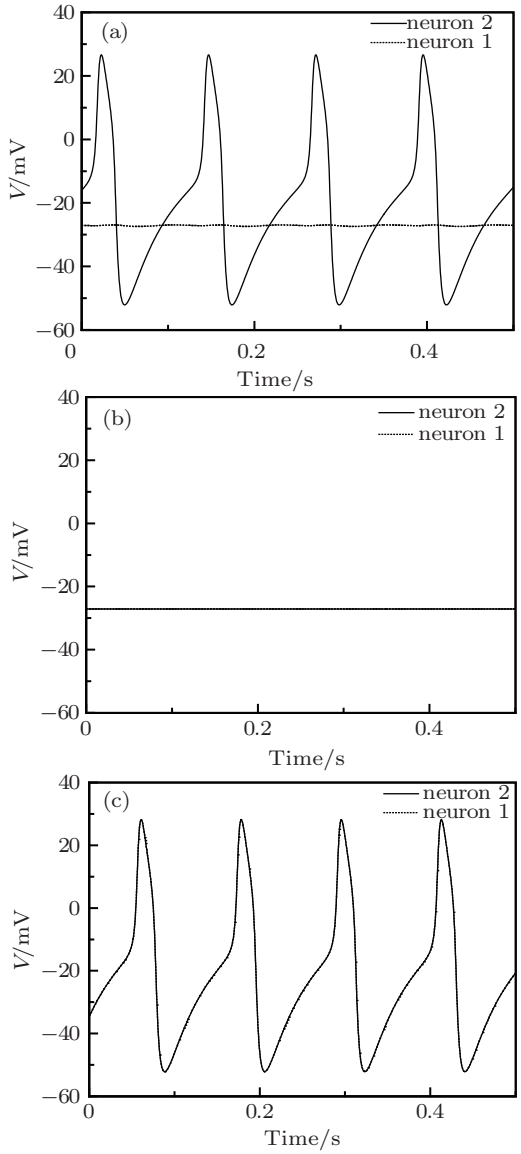


Fig. 6. Synchronization states of the two coupled neurons with initial values (−27.14102, 0.12535) and (1.36163, 0.21568) when $I = 88.4$. (a) Non-synchronization when g_c =0.0003; (b) complete synchronization of the resting condition when g_c =0.03; (c) complete synchronization of period-1 firing when $g_c = 0.5$.

4.1.2. Synchronization transition to complete synchronization of resting condition

When the initial values of neurons 1 and 2 are taken as (−27.14102, 0.12535) and (−19.19939, 0.14056), respectively, the two coupled neurons manifest the transition from non-synchronization ($0.0 < g_c \leq 0.0004$) to complete synchronization of period-1 firing ($0.0004 < g_c \leq 1$) with increasing g_c, as shown in Fig. 7. The non-synchronization behaviors when $g_c = 0.003$ and the complete synchronization of the resting condition when $g_c = 0.5$ are similar to those shown in Fig. 6.

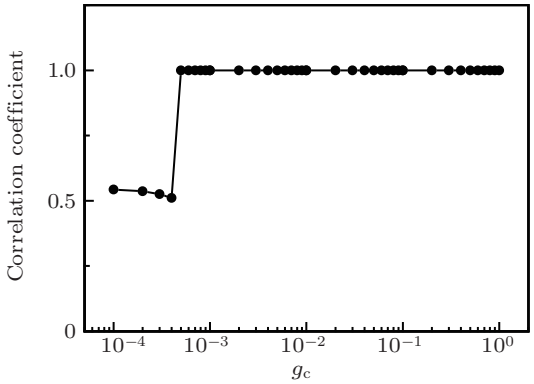


Fig. 7. Correlation coefficient between the two coupled neurons with initial values (−27.14102, 0.12535) and (−19.19939, 0.14056) with g_c increasing when $I = 88.4$.

4.1.3. Initial value-dependent complete synchronization

When $g_c = 0.5$, the complete synchronization can be of either period-1 firing when the initial value of period-1 firing is (1.36163, 0.21568) or resting condition when the initial value of period-1 firing neuron is (−19.19939, 0.14056). The dependence of complete synchronization on the initial values of period-1 firing is as follows.

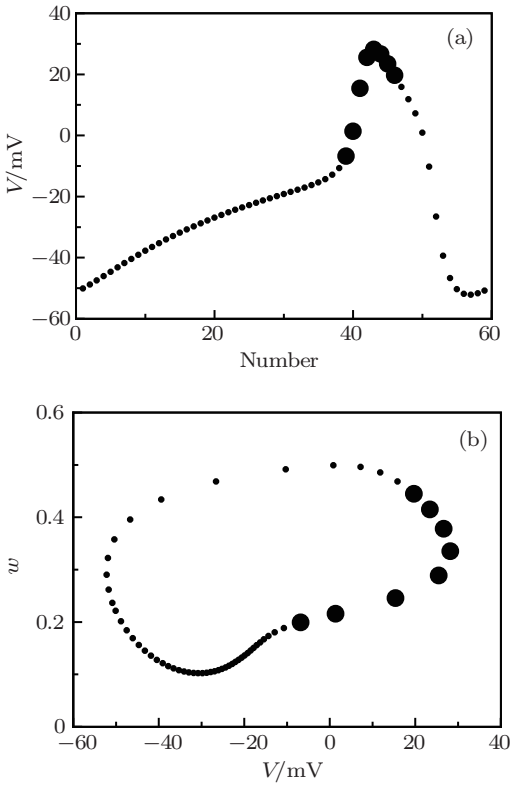


Fig. 8. The initial values within a period of the stable limit cycle of period-1 firing that lead to the complete synchronization of the resting condition (smaller cycle points) and the complete synchronization of period-1 firing (larger cycle points) when $I = 88.4$. Time interval between two continuous points is 2 ms.

As shown in Fig. 8, 59 initial values of period-1 firing neuron are chosen within a period of the stable limit cycle of period-1 firing with time interval 2 ms and the first values were $(-50.08395, 0.22133)$. The time series of initial values of V and discrete points of (V, ω) lying in the trajectory of period-1 firing are shown in Figs. 6(a) and 6(b), respectively. The initial value of the resting neuron is chosen to be identical to the stable equilibrium point $(-27.14102, 0.12535)$. When $g_c = 5$, the 39th–46th initial values (larger cycle points) shown in Fig. 8 lead to the complete synchronization of period-1 firing, while 1st–38th and 47th–59th ones (smaller cycle points) lead to the complete synchronization of the resting condition.

4.2. $I = 89.5$

4.2.1. Synchronization transition to complete synchronization of period-1 firing

When the initial value of period-1 firing neuron is $(-48.65168, 0.37861)$ and of the resting neuron is $(-26.76724, 0.12811)$, the behavior of the coupled neurons is from non-synchronization ($0 < g_c \leq 0.006$), to the complete synchronization of the resting condition ($0.006 < g_c \leq 0.1$), and to the complete synchronization of period-1 firing ($0.1 < g_c \leq 1$), as shown in Fig. 9.

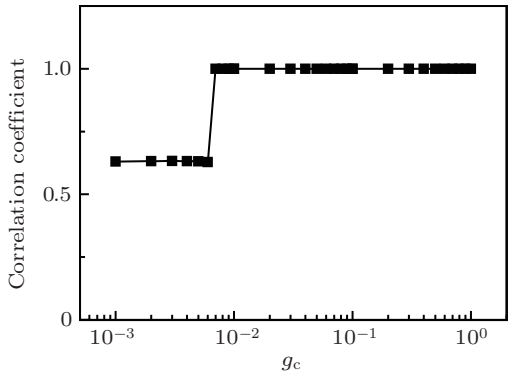


Fig. 9. Correlation coefficient between the two coupled neurons with initial values $(-26.76724, 0.12811)$ and $(-48.65168, 0.37861)$ with g_c increasing when $I = 89.5$.

Non-synchronization of the two coupled neurons when $g_c = 0.005$ is shown in Fig. 10(a). The firing neuron exhibits firing behavior and the resting neuron manifests subthreshold oscillation. The complete synchronization of the resting condition when $g_c = 0.05$ and the complete synchronization of period-1 firing when $g_c = 0.5$ are shown in Figs. 10(b) and 10(c), respectively.

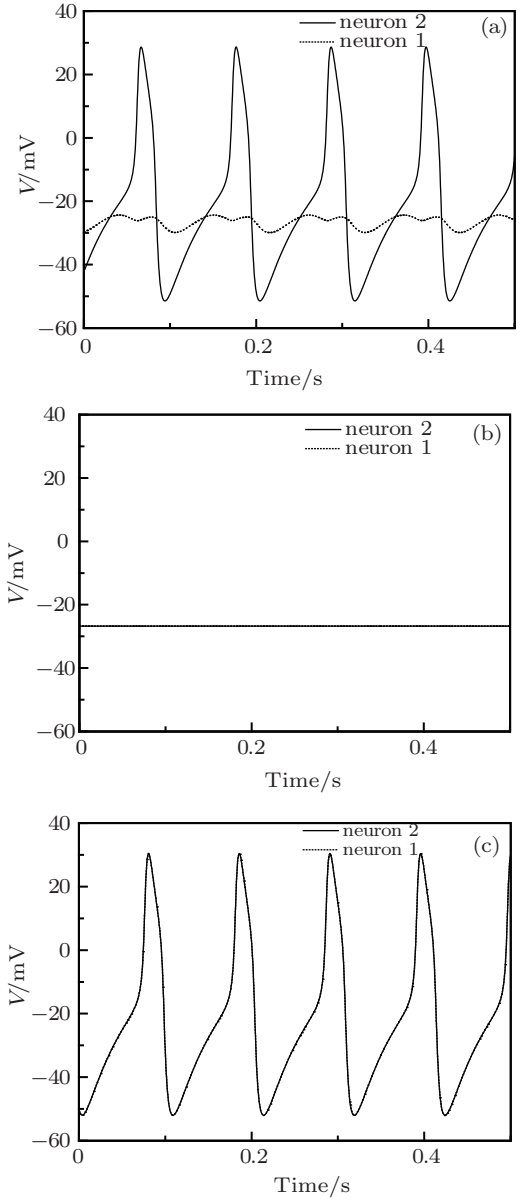


Fig. 10. Synchronization states of the two coupled neurons with initial values $(-26.76724, 0.12811)$ and $(-48.65168, 0.37861)$ when $I = 89.5$. (a) Non-synchronization when g_c =0.005; (b) complete synchronization of the resting condition when g_c =0.05; (c) complete synchronization of period-1 firing when $g_c = 0.5$.

4.2.2. Synchronization transition to the complete synchronization of the resting condition

When the initial value of period-1 firing neuron is $(-30.55347, 0.10361)$, the behavior of the coupled system is from the non-synchronization ($0 < g_c \leq 0.008$) to the complete synchronization of the resting condition ($0.008 < g_c \leq 1$), as shown in Fig. 11. The non-synchronization and the complete synchronization of the resting condition are similar to those shown in Figs. 11(a) and 11(b), respectively.

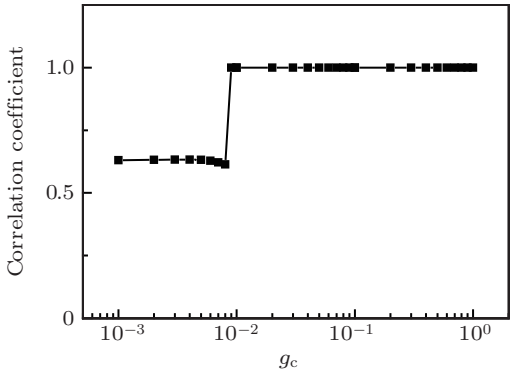


Fig. 11. Correlation coefficient of the two coupled neurons with initial values (−26.76724, 0.12811) and (−30.55347, 0.10361) with g_c increasing when $I = 89.5$.

4.2.3. Initial value-dependent complete synchronization

When $g_c = 0.5$, the complete synchronization can be of either period-1 firing when the initial value of period-1 firing neuron is (−48.65168, 0.37861) or the resting condition when the initial value is (−30.55347, 0.10361). The dependence of complete synchronization on the initial values is as follows.

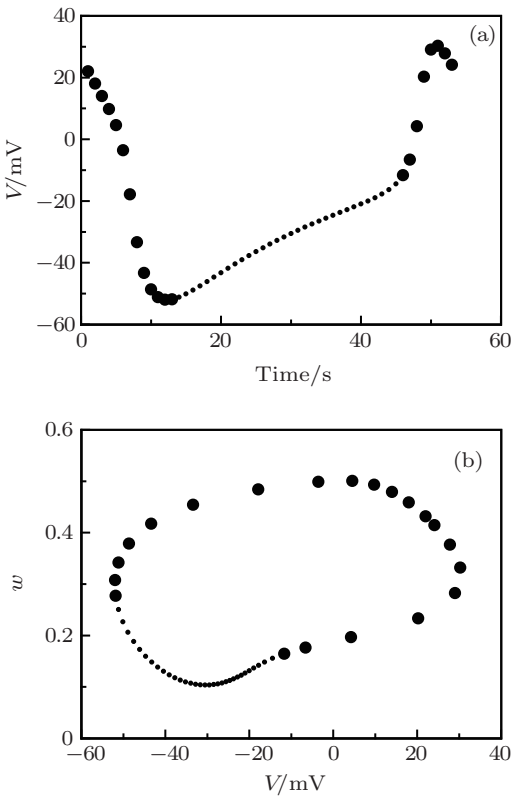


Fig. 12. The initial values within a period of the stable limit cycle of period-1 firing that lead to the complete synchronization of the resting condition (smaller cycle points) and the complete synchronization of period-1 firing (larger cycle points) when $I = 89.5$. Time interval between two continuous points is 2 ms. (a) Spike train and (b) trajectory.

The first initial value of the period-1 firing neuron is chosen as (22.00802, 0.43173) and the subsequent 52 initial values within a period of the stable limit cycle of period-1 firing with time interval 2 ms are shown in Fig. 10. The initial value of the resting neuron is chosen as a value identical to the stable equilibrium point (−26.76724, 0.12811). When $g_c = 5$, 14th–45th initial values (larger cycle points) lead to the complete synchronization of period-1 firing, while 1st–13th and 46th–53th ones (smaller cycle points) lead to the complete synchronization of the resting condition, as shown in Fig. 12.

4.3. $I = 93$

4.3.1. Synchronization transition to the complete synchronization of period-1 firing

When the initial value of the firing neuron is (−39.58738, 0.13392) and of the resting neuron is

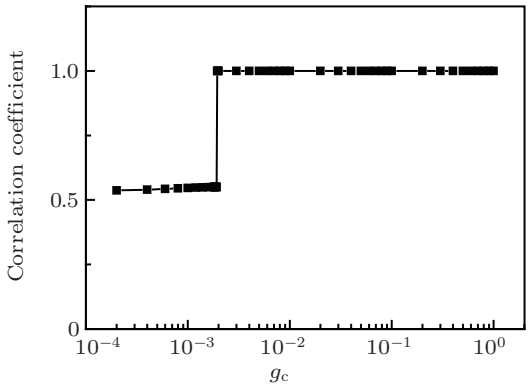


Fig. 13. Correlation coefficient between the two coupled neurons with initial values (−25.56721, 0.13731) and (−39.58738, 0.13392) with g_c increasing when $I = 93$.

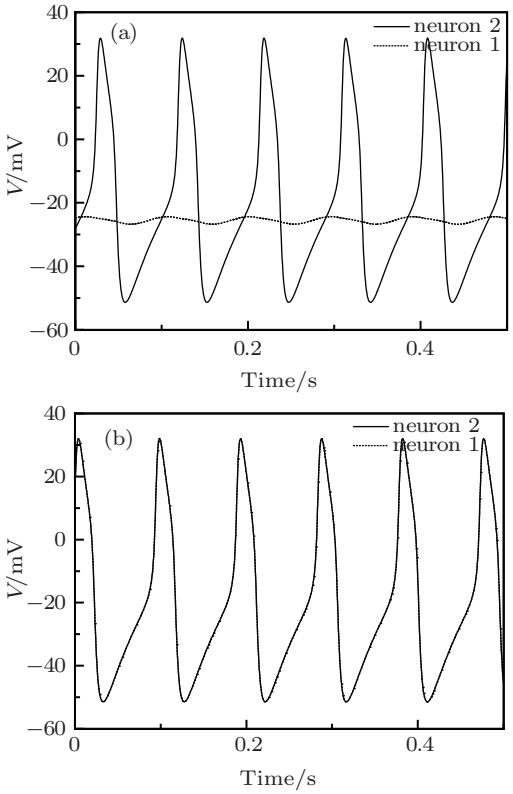


Fig. 14. Synchronization states of the two coupled neurons with initial values (−25.56721, 0.13731) and (−39.58738, 0.13392) when $I = 93$. (a) Non-synchronization when $g_c = 0.0009$; (b) complete synchronization of period-1 firing when $g_c = 0.5$.

(−25.56721, 0.13731), the behavior of the coupled system is from non-synchronization ($0 < g_c \leq 0.00192$) to complete synchronization of period-1 firing ($0.00192 < g_c \leq 1$), as shown in Fig. 13.

The non-synchronization of the two coupled neurons when g_c =0.0009 is shown in Fig. 14(a). Neuron 1 manifests subthreshold oscillation and neuron 2 exhibits firing. The complete synchronization of period-1 firing when $g_c = 0.5$ is shown in Fig. 14(b).

4.3.2. Complete synchronization

The initial value of the resting neuron is chosen as (−25.56721, 0.13731), which is identical to the value of the stable equilibrium point. The first initial value of the period-1 firing neuron is chosen as (−51.4513, 0.30603) and the subsequent 47 initial values within a period of the stable limit cycle of period-1 firing with a time interval of 2 ms are shown in Fig. 15. When $g_c = 0.5$, all 48 initial values lead to the complete synchronization of period-1 firing.

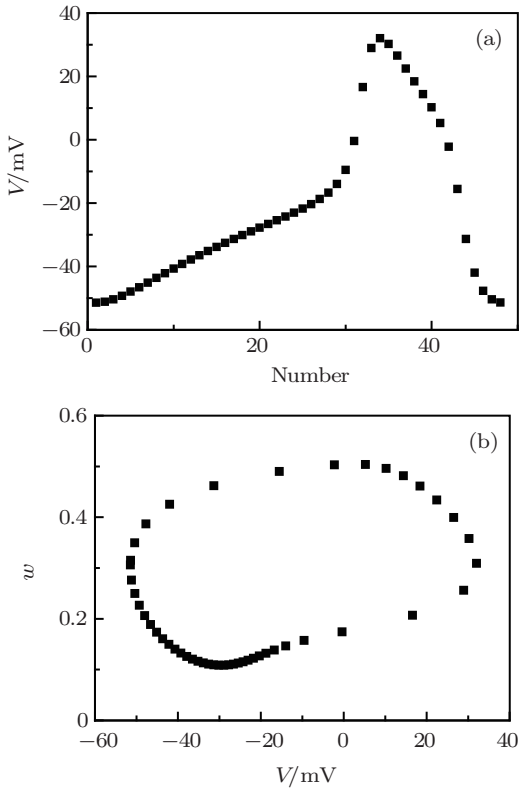


Fig. 15. The initial values within a period of the stable limit cycle of period-1 firing that lead to the complete synchronization of period-1 firing when $I = 93$. Time interval between two continuous points is 2 ms. (a) Spike train and (b) trajectory.

4.4. The dependence of complete synchronization on the initial value

When $I = 88.4$, $I = 89.5$, and $I = 93$, the probability of the initial values of period-1 firing that lead to the complete synchronization of period-1 firing are $8/59 \approx 13.6\%$, $32/53 \approx 60.4\%$, and $48/48 = 100\%$, respectively. With bifurcation parameter I increasing, the probability of the initial values leading to the complete synchronization of period-1 firing increases, correspondingly, the probability of the initial values leading to the complete synchronization of the resting condition decreases. The changing trends of the probability of initial values with respect to the bifurcation parameter are similar to those of the attraction domain.

5. Conclusion and discussion

Synchronization behaviors of the coupled systems with coexisting behaviors are one of the important issues.[19,21–23,26] In the two coupled neurons with co-existing behaviors near a sub-critical Hopf bifurcation point, one neuron is chosen as the resting condition and the other as the period-1 firing. Different synchronization states including non-synchronization and complete synchronization are simulated, dependent on the bifurcation parameter, the initial values of the two neurons and the coupling strength. With the increase of the coupling strength, the synchronization transition process from non-synchronization to compete synchronization is dependent on the bifurcation parameter value and initial values. The complete synchronization states corresponding to a strong coupling strength are dependent on both the bifurcation parameter and the initial values. If the coexisting behavior is close to the resting condition, the complete synchronization can be of either the resting condition or period-1 firing. The probability of the initial value locating at the stable limit cycle within a period of the period-1 firing that leading to the complete synchronization of the period-1 firing is higher than that leading to the complete synchronization of the resting condition. With the increase of the bifurcation parameter value, the probability of the initial values within a period of the stable limit cycle of the period-1 firing leading to complete synchronization of the resting condition decreases while that leading to complete synchronization of period-1 firing increases. The dependence of the complete synchronization on the initial values resembles that of the attraction domain with changing bifurcation parameter. The results are instructive to understand synchronization behaviors of the coupled system with coexisting behaviors.

When the coupling strength is large, the complete synchronization behaviors of the two coupled neurons are dependent on the initial values, showing that the synchronization behaviors manifest coexisting behaviors. Stochastic or coherence resonances have been identified appearing at the coexisting condition.[41] When noise is introduced, stochastic behaviors transiting between the coexisting states and an optimal cooperation between the system and noise are induced. This maybe one of the important potential factors that can lead to complex spatiotemporal behaviors in the real nervous system. In addition, chemical coupling between neurons, heterogeneous neurons and multiple neurons are also important fac-

tors which can induce complex spatio-temporal behaviors and need to be studied further.

Compared with the numerous numerical simulations, there exist far fewer investigations of the bifurcation analysis to the coupled system. The bifurcation of equilibrium of the coupled system has been studied,[42] while the bifurcation of periodic behavior has not been investigated, due to the difficulty of the bifurcation analysis to the limit cycle in the autonomous system.[43] In the present study, the existences and possible bifurcations of the equilibrium of the coupled system are also investigated. When $g_c \geq 0$, an equilibrium E_{00} of the coupled system, related to E_0 of the single neuron model, is identified. As g_c is increased from zero, the equilibrium E_{00} that is determined by the stable E_0 remains stable and no bifurcation happens. The complete synchronization of the rest condition corresponding to the stable E_{00} can be achieved with a suitable g_c. In addition, no other equilibrium different from the equilibrium E_{00} has been identified in the couple system when $g_c \geq 0$. Like E_{00} related to E_0, there exists a stable period-1 firing in the coupled system, related to the coexisting one of the single neuron model, due to the symmetry of the coupled system. The complete synchronization of the period-1 firing is achieved when g_c is chosen as a suitable value. In fact, the complete synchronization of the resting condition and the period-1 firing can be achieved at different initial values, showing that the rest condition and period-1 firing are the coexisting behaviors of the coupled system. When g_c was small, the non-synchronization behaviors manifest the non-resting condition or non-period-1 firing. The bifurcations underlying the non-synchronization behavior and the transition between synchronization states need to be further studied.

In the previous studies, the synchronization transition of the two coupled neurons with coexisting spiking and bursting was primarily investigated.[28,40] In the present paper, the synchronization behaviors of the two coupled neurons with coexisting resting condition and period-1 firing are investigated. The parameter-dependent synchronization transition and initial value-dependent complete synchronization are the focus, manifesting synchronization behaviors more complex than the coupled neurons with monostable behavior. The synchronization transition of the coupled system with monostable behavior are not influenced by the initial values. In future, synchronization behaviors of the two coupled neurons with other kinds of coexisting behaviors should be further investigated to identify more complex synchronization behaviors in nonlinear systems. In addition, the behaviors of neurons in many different parts of the central nervous system are type II excitability corresponding to the subcritical Hopf bifurcation. The synchronization behaviors of the coupled system with more neurons and synaptic connections, which resemble the actual nervous system, should be investigated to reveal the spatiotemporal dynamics similar to those observed in actual nervous systems.

References

[1] Arenas A, Díaz-Guilera A, Kurths J, Moreno Y and Zhou C S 2008 *Phys. Rep.* **469** 93
[2] Boccaletti S, Kurths J, Osipov G, Valladares D L and Zhou C S 2002 *Phys. Rep.* **366** 1
[3] Wang C N, Ma J, Tang J and Li Y L 2010 *Commun. Theor. Phys.* **53** 382
[4] Ma J, Huang L, Wang C N and Pu Z S 2013 *Commun. Theor. Phys.* **59** 233
[5] Wu X and Ma J 2013 *PLoS ONE* **8** e55403
[6] Sun X J, Lei J Z, Perc M, Kurths J and Chen G R 2011 *Chaos* **21** 016110
[7] Zhang N, Zhang H M, Liu Z Q, Ding X L, Yang M H, Gu H G and Ren W 2009 *Chin. Phys. Lett.* **26** 110501
[8] Yuan L, Liu Z Q, Zhang H M, Yang M H, Wei C L, Ding X L, Gu H G and Ren W 2011 *Chin. Phys. B* **20** 020508
[9] Li Y Y, Zhang H M, Wei C L, Yang M H, Gu H G and Ren W 2009 *Chin. Phys. Lett.* **26** 030504
[10] Tang Z, Li Y Y, Xi L, Jia B and Gu H G 2012 *Commun. Theor. Phys.* **57** 61
[11] Liu Z Q, Zhang H M, Li Y Y, Hua C C, Gu H G and Ren W 2010 *Physica A* **389** 2642
[12] Li Y Y, Zhang H M, Wei C L, Yang M H, Gu H G and Ren W 2009 *Chin. Phys. Lett.* **26** 030504
[13] Singer W and Gray C M 1995 *Annu. Rev. Neurosci.* **18** 555
[14] Llinas R and Ribary U 1993 *Proc. Natl. Acad. Sci. USA* **90** 2078
[15] Hartline D K and Gassie D V 1979 *Biol. Cybern.* **33** 209
[16] Buzsaki G and Draguhn A 2004 *Science* **304** 1926
[17] Choi J W, Jung K Y, Kim C H and Kim K H 2010 *Neurosci. Lett.* **468** 156
[18] Gray C M, König P, Engel A K and Singer W 1989 *Nature* **338** 334
[19] Fujisaka H and Yamada T 1983 *Prog. Theor. Phys.* **69** 32
[20] Kim K H, Yoon J, Kim J H and Jung K Y 2008 *Brain Res.* **1236** 105
[21] Pisarchik A N, Jaimes-Reátegui R, Villalobos-Salazar J R, Garcia-Lopez J H and Boccaletti S 2006 *Phys. Rev. Lett.* **96** 244102
[22] Pisarchik A N, Jaimes-Reátegui R and García-López J 2008 *Phil. Trans. R. Soc. A* **366** 459
[23] Ruiz-Oliveras F R and Pisarchik A N 2009 *Phys. Rev. E* **79** 016202
[24] Izhikevich E M 2000 *Int. J. Bifurc. Chaos* **10** 1171
[25] Zhang Y, Tan K K and Lee T H 2003 *Neural Comput.* **15** 639
[26] Zhang Y and Tan K K 2004 *IEEE Trans. Neural Netw.* **15** 329
[27] Tateno T and Pakdaman K 2004 *Chaos* **14** 511
[28] Wang Q Y, Duan Z S, Feng Z S, Chen G R and Lu Q S 2008 *Physica A* **387** 4404
[29] Fröhlich F and Bazhenov M 2006 *Phys. Rev. E* **74** 031922
[30] Cymbalyuk G and Shilnikov A 2005 *J. Comput. Neurosci.* **18** 255
[31] Gu H G, Yang M H, Li L, Liu Z Q and Ren W 2003 *Phys. Lett. A* **319** 89
[32] Yang M H, Liu Z Q, Li L, Xu Y L, Liu H J, Gu H G and Ren W 2009 *Int. J. Bifurc. Chaos* **19** 453
[33] Gu H G, Ren W, Lu Q S, Wu S G and Chen W J 2001 *Phys. Lett. A* **285** 63
[34] Gu H G, Zhang H M, Wei C L, Yang M H, Liu Z Q and Ren W 2011 *Int. J. Mod. Phys. B* **25** 3977
[35] Guttman R, Lewis S and Rinzel J 1980 *J. Physiol.* **305** 377
[36] Lechner H A, Baxter D A, Clark J W and Byrne J H 1996 *J. Neurophysiol.* **75** 957
[37] Tateno T, Harsch A and Robinson H P C 2004 *J. Neurophysiol.* **92** 2283
[38] Prescott S A, Ratté S, Koninck Y D and Sejnowski T J 2008 *J. Neurophysiol.* **100** 3030
[39] Ruiz-Oliveras F R and Pisarchik A N 2009 *Phys. Rev. E* **79** 016202
[40] Gu H G, Li Y Y, Jia B and Chen G R 2013 *Physica A* **392** 3281
[41] Lindner B, García-Ojalvo J, Neiman A and Schimansky-Geier L 2004 *Phys. Rep.* **392** 321
[42] Wang H X, Wang Q Y, Lu Q S and Zheng Y H 2013 *Cogn. Neurodyn.* **7** 121
[43] Ding X L, Li Y Y, Li Q H, Gu H G and Ren W 2009 *J. Dyn. Control.* **7** 297